

# Noncontact scanning force microscopy based on a modified tuning fork sensor

Hagen Göttlich and Robert W. Stark

*Universität München, Institut für Kristallographie und Angewandte Mineralogie, Theresienstr. 41, 80333 München, Germany*

Johannes D. Pedarnig

*Angewandte Physik, Universität Linz, Altenberger Strasse 69, A-4040 Linz, Austria*

Wolfgang M. Heckl<sup>a)</sup>

*Universität München, Institut für Kristallographie und Angewandte Mineralogie, Theresienstr. 41, 80333 München, Germany*

(Received 16 March 2000; accepted for publication 7 April 2000)

Distance control using a tuning fork setup for the detection of shear forces is a standard configuration in scanning near-field optical microscopy (SNOM). Based on this concept, a modified sensor was developed, where a standard silicon tip for atomic force microscopy (AFM) is attached to the front end of one prong of a 100 kHz quartz tuning fork oscillator. Comparison of force curves of a standard tapping-mode AFM cantilever, a conventional fiber tip SNOM sensor and the novel AFM tip shear force sensor demonstrate an enhanced stability and sensitivity of the new sensor. Due to the rigid sensor design the force curves of the AFM tip shear force sensor indicate a perfect noncontact behavior under normal conditions in air. Noncontact images show a comparable resolution to conventional force microscopy. © 2000 American Institute of Physics.

[S0034-6748(00)02708-8]

## I. INTRODUCTION

Atomic force microscopy (AFM)<sup>1</sup> has been used extensively to investigate structural, mechanical and chemical characteristics of surfaces from a wide spectrum of inorganic and organic materials.<sup>2-4</sup> In order to establish well defined and low probing forces a sharp tip, a strongly distance dependent tip sample interaction and a fast response of the controlled distance signal are essential for all AFM operation modes.

Here, we report on the preparation and setup of a fast and sensitive shear force sensor for noncontact atomic force microscopy which combines the advantages of the integrated tip as commonly used in AFM with the rigidity of a quartz tuning fork. This AFM tip shear force sensor was characterized by force curve measurements. Its specific features and their effects on stability and sensitivity are discussed in comparison to corresponding force curves of a commercial AFM cantilever driven in tapping mode and an optical fiber tip shear force sensor. In order to prove its abilities for noncontact imaging, several test samples were investigated in amplitude and in phase signal feedback.

## II. EXPERIMENTAL SETUP

Our AFM tip tuning fork sensor is based on the principle of distance control by shear force detection<sup>5</sup> using a 100 kHz quartz tuning fork oscillator. This allows for higher sensitivity and faster response time in shear force detection than the

normally used 33 kHz oscillator.<sup>6-8</sup> A detailed investigation of the use of the 100 kHz tuning fork is published elsewhere.<sup>9</sup>

For the experiments a modified commercial near-field optical microscope<sup>10</sup> was used, which was operated in scanning shear force mode. The modifications allowed for stable feedback operation for both amplitude and phase of the piezoelectric signal of the 100 kHz quartz tuning fork oscillator. A silicon tip of a commercial AFM cantilever<sup>11</sup> served as force pickup. Figure 1 shows schematically and as photograph a close-up of the composite sensor. The cantilever is glued<sup>12</sup> onto the front end of one prong of the quartz tuning fork.<sup>13</sup> The fork was mounted perpendicular to the sample surface and resonantly excited by a dither piezo.<sup>14</sup>  $Q$  values of  $\sim 1000$  and  $\sim 5000$  were measured in air for the composite sensor and the bare oscillator, respectively. From interferometric measurements a tip vibration amplitude of  $\sim 0.3$  nm and a mean damping force of the sensor in air of  $\sim 2$  nN were derived.<sup>9</sup> For small distances the tip vibration parallel to the sample surface was damped additionally by shear forces modifying the piezoelectric signal. The fork signal was preamplified using a current-voltage converter (I-VC) with a gain of  $8 \times 10^7$  V/A at 100 kHz. The preamplifier output was demodulated by a lock-in amplifier<sup>15</sup> with integration times in the range from 30 to 100  $\mu$ s. An analog coordinate converter was used to derive amplitude and phase of the piezoelectric signal from the fast ‘‘x-y’’ lock-in output. For distance control the amplitude or phase signal was fed into the feedback loop.

<sup>a)</sup>Author to whom correspondence should be addressed; electronic mail: w.heckl@lrz.uni-muenchen.de

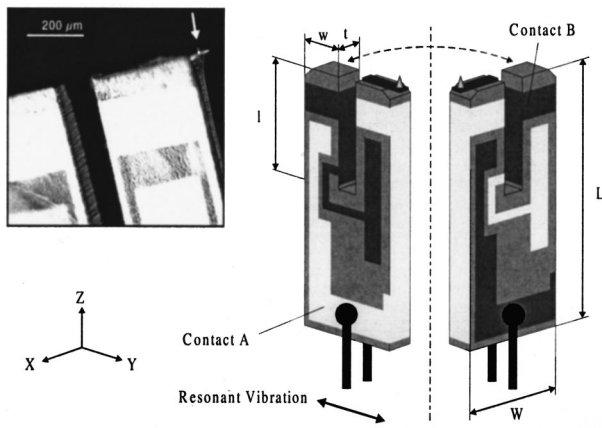


FIG. 1. Schematic close-up of the AFM tip shear force sensor. An optical photograph of the composite sensor is shown as inset (white arrow marks the silicon tip).

### III. RESULTS AND DISCUSSION

In order to determine the dynamic distance behavior of the AFM tip shear force sensor and to allow comparison with conventional force sensors, force curves have been recorded on freshly cleaved mica in ambient conditions. Amplitude and phase data were measured simultaneously. Figure 2 shows characteristic approach/retraction cycles of a regular AFM cantilever taken in tapping mode operation. The amplitude signal [Fig. 2(a)] vanishes completely within a 15 nm tip sample interaction zone. It can be divided into three parts.<sup>16</sup> In the noncontact zone above the hatched space the vibration of the cantilever is damped by long-range attractive tip sample interactions. The quasicontract or tapping zone below the hatched space is mainly ruled by repulsive forces. Here, the tip touches the sample surface mechanically. Both zones show a continuous, almost linear decrease of the amplitude with  $z$ . The intermediate region (hatched space) describes the transition from attractive to repulsive damping forces. It exhibits a bistable behavior which is critically dependent on surface chemistry and therefore cannot be used for reliable feedback regulation. The slope of the phase signal in Fig. 2(b) changes the sign over the full response range

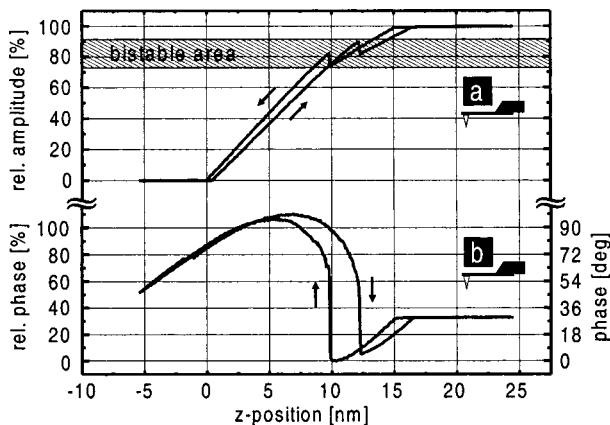


FIG. 2. Force curves of a standard AFM cantilever operating in tapping mode: (a) amplitude signal normalized to maximum value, (b) phase signal normalized to 90°, which corresponds to an amplitude value of 100%.

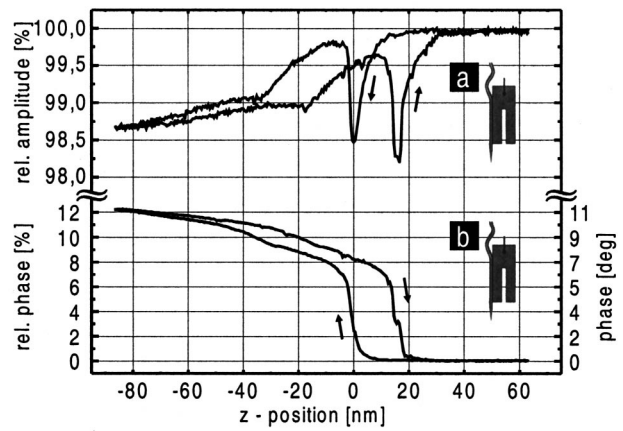


FIG. 3. Force curves of a conventional fiber tip SNOM sensor: graphics (a) and (b) according to Fig. 2.

in  $z$  and is therefore not appropriate for distance control. Thus, true noncontact can hardly be achieved by a conventional cantilever in ambient conditions.

A different behavior could be observed for fiber sensors as used in optical near-field microscopy (i.e., the fiber is attached to one prong of a 100 kHz tuning fork and vibrates parallel to the sample surface<sup>9</sup>). The experimental amplitude-distance relation in Fig. 3(a) shows a linear decrease of amplitude, when the fiber approaches the surface. However, when the fiber tip is in contact with the sample surface ( $z=0$ ), the oscillation amplitude does not vanish. In contrast, the amplitude increases significantly and decreases again, when the tip is pressed stronger into the sample. This behavior is caused by the elasticity of the glass fiber protruding from the fork prong by about 0.3 mm. Another effect of the high sensor elasticity is the small total decrease of the amplitude signal of  $\Delta A_{tot} \approx 1.4\%$ . This leads to a maximum change of the signal of  $(\Delta A/\Delta z)_{max} \approx 0.2\%/nm$ , which is more than one order of magnitude lower as in the case of the tapping mode AFM cantilever, where the maximum change of the amplitude signal amounted to 8%/nm [Fig. 2(a)]. Because of its rather poor sensitivity and its nonmonotonic behavior at the tip sample touch point the amplitude signal of

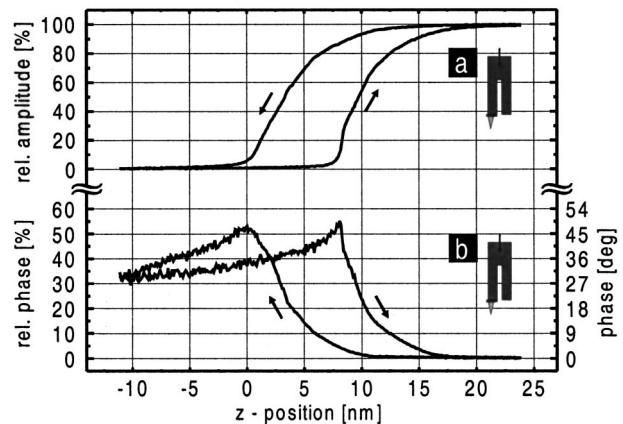


FIG. 4. Force curves of the modified shear force sensor with AFM tip: graphics (a) and (b) according to Fig. 2.

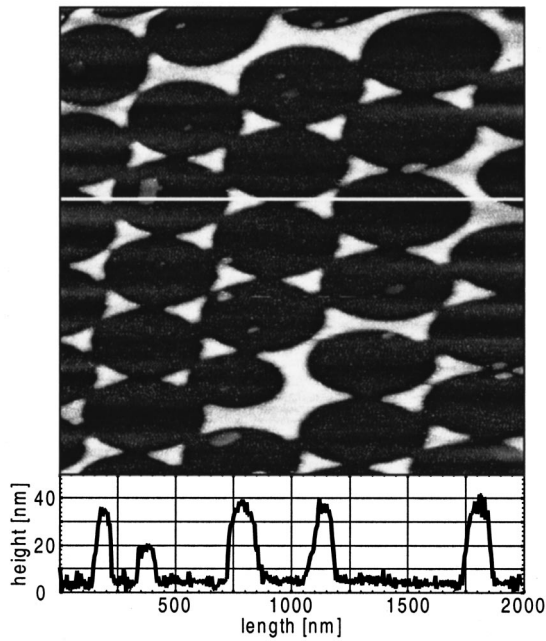


FIG. 5. Amplitude controlled topographical shear force image of aluminum/glass pattern (scan rate  $2 \mu\text{m/s}$ , unfiltered). White lines mark the cross section in the graphs below.

the fiber sensor allows a reliable distance control for large tip sample distances only.

In contrast to all signals mentioned above, the phase signal of the fiber sensor [Fig. 3(b)] is monotonic, ensuring a stable control over the full  $z$  range of probe sample interaction. The signal change of the phase is higher as compared to the amplitude signal in Fig. 3(a). It provides with a maximum value of  $(\Delta\varphi/\Delta z)_{\text{max}} \approx 1.2\%/nm$  a much improved sensitivity. Furthermore, the phase signal offers shorter response times.<sup>8</sup> These results demonstrate, that in the case of the fiber tip shear force sensor, the phase signal should be the preferred signal for distance control.

The amplitude of our AFM tip shear force sensor in Fig. 4(a) reveals a superior signal change [ $(\Delta A/\Delta z)_{\text{max}} \approx 12\%/nm$ ] as compared to the conventional fiber tip shear force sensor. The signal decreases continuously. Unlike both other sensor types mentioned above, there are no critical bistable regions. The phase signal [Fig. 4(b)] shows a monotonic increase of the phase angle in the noncontact regime. The maximum signal change is  $(\Delta\varphi/\Delta z)_{\text{max}} \approx 8\%/nm$ .

The steady shape of both plots, without changes in the sign of the slope, demonstrate the high stability of the AFM tip shear force sensor for both signals. The main advantages of the AFM tip shear force sensor are its high sensitivity to the tip sample separation and its well defined tip vibration on an angstrom scale due to a rigid sensor design. The probing forces are  $< 100 \text{ pN}$  at distances of  $\geq 10 \text{ nm}$ .<sup>9</sup>

As mentioned above, the phase signal is usually preferred for distance control, because it offers faster response times. However, there is the need to use the amplitude signal for distance regulation in experiments, where chemical properties of the sample are investigated.<sup>17</sup> Employing the amplitude signal for distance regulation potentially allows the use of the phase signal for additional image information. Thus,

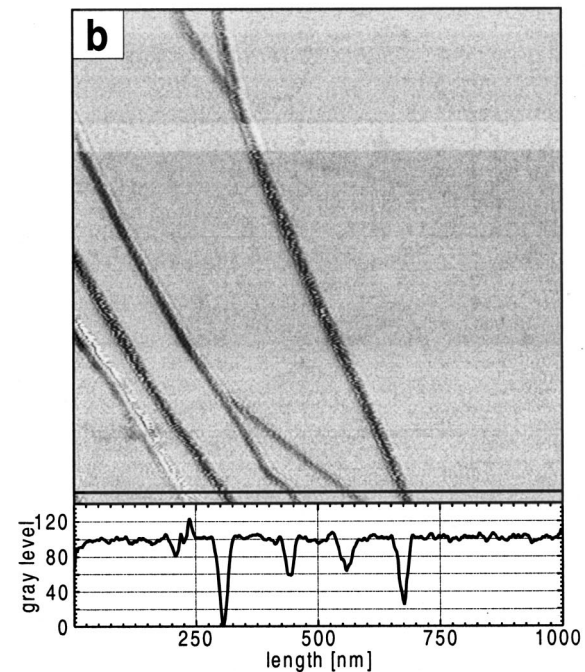
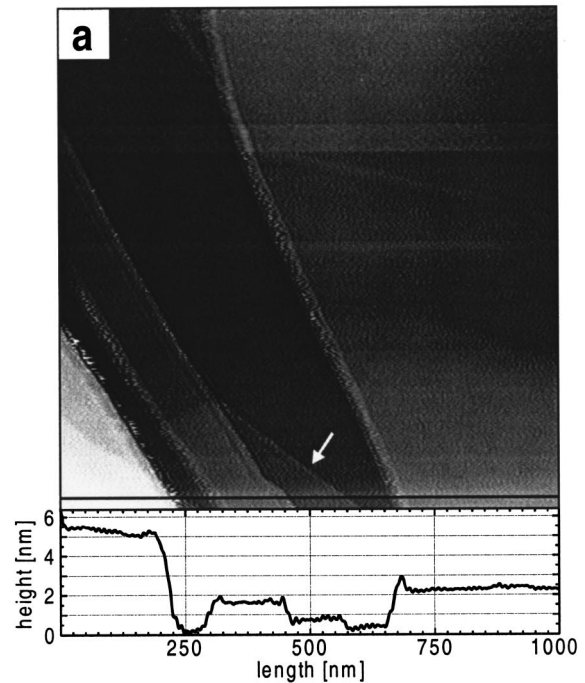


FIG. 6. Shear force images of multilayer steps on a HOPG surface (scan rate  $2 \mu\text{m/s}$ , unfiltered): (a) topographic phase image (note the double step marked by the arrow), (b) amplitude image. Black lines mark the cross section in the graphs below.

there is the option to compare conventional phase-imaging AFM<sup>18,19</sup> with the phase contrast in the new detection scheme.

Different samples were imaged using amplitude or phase signal for distance control. Figure 5 shows an aluminum/glass pattern recorded with amplitude feedback. The lateral resolution of this image is comparable to a standard AFM

image. From cross section analysis a  $z$  resolution of 4 nm was determined.

Figures 6(a) and 6(b) show phase and amplitude images of multilayer steps on a freshly cleaved highly oriented pyrolytic graphite (HOPG) surface. Both images were recorded simultaneously employing the phase signal for distance regulation. In Fig. 6(a) the edge of a graphite double layer (arrow) is prominent. Cross sectional analysis reveals a step height of  $0.7 \pm 0.1$  nm, in good accordance with the literature value of 0.669 nm for the height of a double step.<sup>20</sup> The  $z$  resolution was not limited by the force sensor but by the insufficient sample depth of the electronic A/D converter. The lateral resolution was limited by the piezo driving electronics ( $x$ - $y$  resolution: 1.5 nm). The amplitude image in Fig. 6(b) reproduces all individual features of the phase image and enhances the steps.

Other experiments with the AFM tip shear force sensor proved its suitability for imaging of biological samples under ambient conditions. To verify true noncontact probing in particular, a series of 20 consecutive images of the same features of supercoiled plasmid DNA was recorded. Despite the fragile nature of the macromolecules, no degradation was observed. This leads to the conclusion that imaging was performed in stable noncontact mode without mechanical touching of the sample surface.

The described AFM tip shear force sensor is easy to handle, without the need of adjustment of optical components. It has a well defined distance behavior and therefore a high stability over the full  $z$  range, which offers a valuable advantage to a standard AFM cantilever driven in noncontact tapping mode. Tuning fork vibration amplitudes comparable to atomic lattice constants can be used for imaging. With improved electronic components the oscillation amplitude could be reduced further. Atomic resolution in a shear force

detection scheme is an active field of progress and might become a standard procedure.

## ACKNOWLEDGMENTS

The authors thank the Bundesministerium für Bildung und Forschung (13N7205/6 and 13N7509), the Bayerische Forschungsförderung and the Jubiläumsfonds der Österreichischen National Bank (7796) for financial support.

- <sup>1</sup>G. Binnig, C. F. Quate, and C. Gerber, *Phys. Rev. Lett.* **56**, 930 (1986).
- <sup>2</sup>M. Radmacher, M. Fritz, and P. K. Hansma, *Biophys. J.* **69**, 264 (1995).
- <sup>3</sup>R. W. Stark, T. Drobek, M. Weth, J. Fricke, and W. M. Heckl, *Ultramicroscopy* **75**, 161 (1998).
- <sup>4</sup>C. D. Frisbie, L. F. Rozsnyai, A. Noy, M. S. Wrighton, and C. M. Lieber, *Science* **265**, 2071 (1994).
- <sup>5</sup>E. Betzig, P. L. Finn, and J. S. Weiner, *Appl. Phys. Lett.* **60**, 2484 (1992).
- <sup>6</sup>P. Günther, U. C. Fischer, and K. Dransfeld, *Appl. Phys. B: Photophys. Laser Chem.* **48**, 89 (1989).
- <sup>7</sup>K. Karrai and R. D. Grober, *Appl. Phys. Lett.* **66**, 1842 (1995).
- <sup>8</sup>A. G. T. Ruiten, J. A. Veerman, K. O. von der Werf, and N. F. van Hulst, *Appl. Phys. Lett.* **71**, 28 (1997).
- <sup>9</sup>J. D. Pedarnig, H. Göttlich, and W. M. Heckl, *Probe Microsc.* **1**, 239 (1998).
- <sup>10</sup>AURORA, TopoMetrix GmbH, Darmstadt, Germany.
- <sup>11</sup>Nanosensors TM, contact, pyramidal tip shape, cone half angle  $\alpha=18^\circ$ , tip curvature radius  $r \leq 10$  nm, tip height  $H=10-15 \mu\text{m}$ , Dr. Olaf Wolter GmbH, Wetzlar, Germany.
- <sup>12</sup>Araldit 395/396, Ciba Geigy, Switzerland.
- <sup>13</sup>MCS-MX1 100 kHz,  $L=3.55$  mm,  $W=0.7$  mm,  $l=1.42$  mm,  $w=0.29$  mm,  $t=0.13$  mm, Micro Crystal Switzerland, Switzerland.
- <sup>14</sup>EBL#2, Staveley Sensors, United Kingdom.
- <sup>15</sup>Model SR 830, Stanford Research, USA.
- <sup>16</sup>B. Anczykowski, D. Krüger, and H. Fuchs, *Phys. Rev. B* **53**, 15485 (1996).
- <sup>17</sup>M. Stark and R. Guckenberger, *Rev. Sci. Instrum.* **70**, 3614 (1999).
- <sup>18</sup>S. N. Magonov, V. Elings, and M. H. Whangbo, *Surf. Sci. Lett.* **375**, L385 (1997).
- <sup>19</sup>R. W. Stark, T. Drobek, and W. M. Heckl, *Appl. Phys. Lett.* **74**, 3296 (1999).
- <sup>20</sup>*Handbook of Chemistry and Physics*, 70th ed., edited by R. C. Weast (Chemical Rubber, Boca Raton, 1989), Vol. E-196.